

Experimental validation of simulation methods for bi-directional transmission properties at the daylighting performance level

Fawaz Maamari¹, Marilyne Andersen², Jan de Boer³, William L. Carroll⁴,
Dominique Dumortier¹, Phillip Greenup⁵

¹ ENTPE, Rue Maurice Audin, 69518 Vaulx en Velin Cedex, France. Current address of F. Maamari: Soft Energy consultants, 4 place Jean Chorel, 69100 Villeurbanne, France.

² Solar Energy and Building Physics Laboratory (LESO-PB), Swiss Federal Institute of Technology (EPFL), Switzerland. Current address: Building Technology Program, Department of Architecture, Massachusetts Institute of Technology (MIT), USA.

³ Fraunhofer-Institut für Bauphysik, Nobelstrasse 12, 70569 Stuttgart, Germany.

⁴ Lawrence Berkeley National Laboratory, University of California, 1 Cyclotron Road, MS 90R3111, Berkeley, CA 94720, USA.

⁵ Arup Australasia, Level 10, 201 Kent St, Sydney NSW 2000, Australia.

* Corresponding Author.

Fawaz Maamari,
Soft Energy Consultants
4 Place Jean Chorel
69100 Villeurbanne,
France
Tel/fax: +33 4 78 89 99 95
E-Mail Address: maamari@alicemail.fr

Abstract

The objective of this paper is to assess the capability of existing lighting simulation methods to predict the performance of complex fenestration systems (CFS), whose potential in daylight and sunlight control make them an increasingly popular alternative to conventional glazing.

The research was conducted in two phases. First, collect reliable reference data by taking illuminance measurements inside a black box under a measured and controlled external luminance distribution, the black-box's only aperture being covered with a complex glazing sample. Two types of materials were used: a SerraglazeTM element and a Laser Cut Panel (LCP).

Several simulation methods were then investigated and validated against this reference case. On one hand, measured BTDF for both material samples were integrated in different simulation tools to determine the resulting indoor lighting conditions under the external luminance distribution chosen for the reference case. The same method was then applied with calculated BTDF data, based on ray-tracing calculations. Finally, one of the CFS (the LCP) was modeled in a backward ray-tracing program so that the inside illuminance distribution could be deduced without requiring BTDF data to be used.

The comparison between the experimental reference data and the simulation results showed that the effect of the CFS on the room's illumination could be predicted with acceptable accuracy for most of the tested methods (generally within 10%-20%). The simplicity of the testing scenarios allowed error sources related to simulation to be highlighted and helped determine the extent to which an accurate physical description of the samples could influence the results. Based on this study, recommendations were made for a better use of existing simulation methods.

Keywords:

Daylight simulation, Bidirectional Transmission Distribution Function (BTDF), Complex Fenestration Systems (CFS), Validation data.

1. Introduction

Since the early nineties, a variety of light redirecting glazing and shading systems, also called Complex Fenestration Systems (CFS), have made their way into commercial buildings, mostly office buildings [1, 2, 3], greatly opening up opportunities for a better daylight distribution and an appropriate sunlight control in the hope of decreasing electric lighting needs and enhancing visual comfort.

Predicting the performance of such systems is one of the main difficulties the lighting simulation domain is facing despite the significant progress observed in this field [2, 4, 5, 6, 7], the light-redirecting properties of the CFS being made even more complex by the variable distribution of sky luminances.

To achieve a reliable modeling of the light propagation in rooms using CFS, the spatial distribution of transmitted daylight must be characterized precisely, in a similar way as for lighting fixtures [8]. This is done by assessing the Bidirectional Transmission (or Reflection) Distribution Function (BTDF, BRDF) of these CFSs, which is defined by the Commission Internationale de l'Éclairage as the “quotient of the luminance of the medium by the illuminance on the medium” [9]. Many efforts are being investigated internationally to propose new experimental methods for assessing the Bi-directional Transmission Distribution Function (BTDF) of CFS as well as alternative simulation approaches based on ray-tracing methods, reviewed in [10]. Predicting the performance of CFS in buildings remains however a critical issue because the amount of publicly available BTDF data is still relatively small [10] and reference experimental BTDF data are not yet available for lack of standards in validation protocols. The reliability of existing BTDF data is therefore strongly dependent on the assessment method and errors have been found to vary between a few percent and 50% or more [10]. In addition, BTDF data must be combined with an accurate description of the sky luminance distribution for indoor illuminance maps to be deduced [11, 12, 13, 14, 15, 16].

This paper describes a comparative study aiming at assessing the capability and accuracy of existing simulation methods in predicting the performance of a CFS. The reference case consisted of a set of illuminance measurements made inside a black-box that included a physical CFS sample in its only aperture, this simple geometry and surface properties being chosen so that uncertainties could be minimized [14]. Two samples of light-redirecting glazing were chosen for this study: a SerraglazeTM sample and a Laser Cut Panel (LCP).

The reference measurements were conducted under an artificial sky and under real sky conditions, the sky luminance distribution being simultaneously assessed in both cases with a CCD camera-based sky scanner. The sky conditions were chosen so as to exclude direct sun and the selected CFS samples were thin and showed small optical features: errors related to near field issues and diffuse reflection could therefore be minimized.

Several simulation methods were then compared and tested against the reference case. They can be categorized in two fundamental approaches depending on how the CFS was modelled: either using a ray-tracing simulation program or using the samples' BTDF data. In the first case, only the LCP was considered, and the full simulation was made in Radiance without requiring any BTDF data. In the second case, three assessment methods were used to produce BTDF values: one relied on measured data (physical samples), the other two on numerical goniophotometers developed using different commercial forward ray-tracing softwares, these goniophotometers differing mainly in the type of virtual detector that was modeled (pyramidal or hemispherical vs. cubical). The various BTDF data sets were then combined with the external luminance distribution to predict the illuminance variation inside the room (black box).

In this paper, the reference experimental set-up is first described and the related uncertainties estimated (section 2). A description of the different BTDF assessment methods considered in this analysis is then given in section 3 together with a discussion on their related error sources.

In section 4, the various simulation algorithms used to calculate the interior illuminance distribution based on BTDF data are presented, as well as the Radiance approach using an analytical model for the LCP. Finally, experimental and numerical results are compared in section 5 and the applicability and limitations of each approach are investigated.

2. Experimental set-up for reference data

To assess the influence of a CFS on the illuminance distribution inside a room, an experimental set-up including a scale model, an artificial sky, a calibrated CCD camera and different photosensors was assembled.

The illuminance variation inside the scale model was measured with and without a CFS sample, placed in an upwards-facing aperture.

2.1 Scale model description

The scale model was developed and used at ENTPE [16]. It consisted of a wooden cubic box of dimensions of 0.8 m × 0.8 m × 0.6 m, representing a room of 4 m × 4 m at a 1:5 scale. Different sizes of vertical or horizontal openings were allowed, but only a 0.2 m × 0.2 m (36 mm deep) roof opening was used for the purpose of this study (see Figure 1 (a)).

All interior surfaces were painted with a matt black paint showing a reflectance of 4.5% ± 1%. The bi-directional reflection aspect of the painted surfaces was measured with a plane goniophotometer and was found to closely fit the Lambertian model (Uniform reflected luminance +/- 10%).

Figure 1

Photocells were positioned inside the scale model at various locations on the floor, wall surfaces (see Figures 4 and 7), and on the opening level for external illuminance measurements (Figure 1(a)).

A CCD camera equipped with a fisheye lens was used to measure the external luminance distribution as seen from the opening surface level; the placement system is illustrated in Figure 1(b).

2.2 Luminance map measurements

One of the main error sources when comparing daylighting simulations to experimental measurements is due to the description of the external sky luminance distribution, whether it refers to a real or an artificial sky. Standardized sky models (CIE overcast sky, uniform sky, etc.) are generally used in simulation to represent this luminance distribution, which can introduce important error sources.

In this paper, the authors were able to minimize related error sources by assessing the external luminance distribution simultaneously with the illuminance measurements performed inside and outside the scale model.

Figure 2

The sky luminance distribution was measured using the Photolux system, which uses a calibrated CCD camera (NikonTM Coolpix model 990) equipped with a fisheye lens in combination with a dedicated software [17]. High-resolution luminance maps (360,000 values) can be produced from one or more images (see Figure 2), multiple exposures being used to avoid saturated or under-exposed zones in the case of high range of luminance variation. As the maximum luminance that can be measured with the Coolpix 990 is close to 50,000 cd/m², the system cannot provide information on the luminance of the sun and its circumsolar region, which was a reason for excluding direct sunlight from this study.

The luminance maps were saved into a Radiance compatible format (regular steps of 1° or 5°) or into an equivalent intensity distribution file using the IESNA format.

The maximum error on measured luminance values was estimated to be about 20%. To reduce this error further, measured values were corrected accounting for the difference between the measured external illuminance and the value that was calculated from the measured luminance map. These corrections made it possible to reduce the error to about 5% excluding highly saturated zones [16].

2.3 Experimental protocols

Two situations were tested, the first with a Serraglaze™ sample under an artificial sky, the second with a Laser Cut Panel (LCP) sample under external real sky.

The main difference between the two scenarios is related to the external luminance distribution: the LCP scenario presented a higher directionality in the sky luminance distribution (see Figure 6), which allowed the light redirecting properties of the material to be highlighted better. The uniformity of the luminance distribution in the Serraglaze scenario allowed testing of the simulation methods with a lower level of complexity.

Another important difference between the two scenarios is related to the dynamic variation of the luminance distribution (stable for the Serraglaze scenario while there were moving irregular clouds for the LCP scenario) and to the possibility of measuring luminance maps simultaneously with illuminance values.

Figure 3.

2.3.1 Serraglaze™

The Serraglaze™ material is an optical device made of two identical crenellated plastic panels facing each other and shifted by half a period to fit into each other (see Figure 3(b)). The resulting thickness of the panel is 7 mm (2.27 mm for each exterior layer, 4.73 for the crenels), the crenels being cut at slightly off-horizontal slopes (3° when edge is full, 1° when edge is cut off at 45°, see Figure 3(b)). These specific geometric features were given by the manufacturer, and were not verified experimentally on the available sample.

The Serraglaze™ scenario was conducted under the artificial sky at ENTPE, which is a 2 m × 2 m × 2.1 m room with four mirror walls and a luminous ceiling. The luminance distribution achieved by the artificial sky approximated the CIE overcast sky model (see Figure 5). The main advantage of using an artificial sky relies in the stability of the luminance distribution over time.

The scale model's roof was situated 1.45 m above the ground. Six measurement points were used inside the model, as shown in Figure 4. The Serraglaze™ sample was positioned at the top of the roof opening (see Figure 1(a)), with linear crenels perpendicular to the line of measurement points.

Figure 4, Figure 5

The illuminance measurements were first made with an empty opening, then with the sample. The roof element was then removed completely and replaced by the camera positioning system to capture pictures of the artificial sky from the center of the opening, thus reducing error sources related to a near field situation [16, 18]. The external illuminance was measured simultaneously with both the image capture and internal measurements so that the stability of the sky luminance level (between the time of the image capture and the time of internal illuminance measurements) could be checked.

The measured internal illuminance values were corrected to account for the difference between measured external illuminance and the one deduced from the luminance map [16].

2.3.2 Laser Cut Panel

The Laser Cut Panel (LCP) is made of an acrylic panel of thickness 6 mm and dimensions 300 x 300 mm, through which a series of parallel cuts were made with a laser beam every 4 mm (the cuts themselves extend over 0.3 mm, see Figure 3(a)).

The LCP scenario was conducted on the roof of ENTPE with negligible surrounding masks and under an intermediate sky condition where the sun was hidden by clouds, as shown in Figure 6. The main advantage of using real sky conditions lies in the variability of the luminance distribution over the sky vault, resulting in a higher illuminance variation inside the scale model, thanks to which the influence of the LCP can be highlighted. Its disadvantage is due to the lack of control of the luminance distribution over time, which is partially compensated by taking pictures and illuminance measurements simultaneously.

The sample was positioned at the top of the roof opening with the panel's cuts perpendicular to the line of measurement points.

Nine measurement points were used inside the model (see Figure 7) in addition to the one for external illuminance.

Illuminance measurements were again first taken with an empty opening, then with the LCP sample. Pictures of the sky luminance distribution were taken simultaneously with each set of measurements. The measured internal illuminance values were corrected to account for the difference between measured external illuminance and external illuminance deduced from the luminance map.

Figure 6, Figure 7

2.4 Estimation of the uncertainties in the reference data

The accuracy of a lighting simulation (compared to experimental data) is first affected by the errors related to the physical description of the scenario components (materials, measurement equipment etc.) [14, 15].

Within this validation context, uncertainties due to inaccurate descriptions of the two scenarios and to the measurement procedures themselves were calculated from identified error sources by using the following relation:

$$U = \sqrt{\sum_i (Error_{(i)})^2} \text{ where } i \text{ is the number of error sources. (Equation 1)}$$

Upper and lower tolerance limits (=measured value + or – the estimated uncertainties) can then be deduced, providing the margins within which simulation results should remain for acceptable accuracy. It must be noted that errors related to the BTDF data are not taken into consideration in these tolerance margins and are described separately in section 3.3.

2.4.1 SerraglazeTM scenarios

For an empty opening under the artificial sky, the measurements' uncertainty was estimated (through equation 1) to +/- 10% taking into consideration the following error sources [16]: photocells calibration, photocells cosine correction, spectral sensibility, flux variation, photocells position, near field effects (described below), surface reflectance (accuracy, homogeneity and directionality), geometry dimensions, and the external luminance distribution. For the measurements with the SerraglazeTM sample, the error sources were similar to the empty opening in addition to an error source related to the positioning of the sample and led to an uncertainty estimated at 13%.

For the hemi-directional transmission, most of the error sources related to the scenario description were avoided or minimized with the exception of the luminance distribution and the positioning of the sample, leading to an uncertainty estimated at 10%.

Figure 8, Figure 9

The near field error source is illustrated in Figure 8 for a bare opening and refers to the difference between the portion of the (artificial) sky vault seen by a measurement point and the corresponding luminance field captured by the camera from the center of the opening (and used to calculate the direct illuminance at the measurement point). In the example shown in Figure 8, the angle of view from sensor position P4 through the opening defines the "real" portion of the

sky seen by this point. This angle is used to delimit the "simulated" portion of the captured sky luminance map, which will be used in the calculation of the direct illuminance at P4. The difference between the luminance distribution inside the "real" and the "simulated" portions is equal to the error assumed in simulation results. Figure 9 shows the influence of this error on the correlation between measured and simulated values (obtained by using the luminance map as a sky description in Radiance). For this study, near field error source was found relatively low thanks to the small size of the opening.

2.4.2 LCP scenario

The difference between this scenario and the previous one is the absence of any near field error source and higher errors related to the luminance map and the sample position, as the luminance distribution presents a higher directionality (See Figure 6).

The resulting uncertainty was estimated using equation (1) and found to be of 10% for the bare opening, 18% for the measurements with the LCP sample and 15% for the hemi-directional transmission.

3. Assessment of BTDFs

Three of the four presented simulation methods in this paper are based on the use of BTDF data. The BTDF data of the tested samples were obtained by means of three different methods: one experimental approach based on digital imaging techniques, and two numerical methods based on ray-tracing techniques. A short description of these methods is given in this section while detailed information can be found in [10].

3.1 Bidirectional video-goniophotometer

The experimental assessment of BTDFs was achieved with a bidirectional goniophotometer based on digital imaging techniques developed at LESO-PB / EPFL. The light flux emerging from the investigated sample shines on a diffusing flat screen, at which a calibrated Charge-Coupled Device (CCD) camera is aiming. The camera is used as a multiple-points luminance-meter. To cover all possible emerging directions (2π steradian), the camera and the screen perform rotations of a 60° angle magnitude. [19, 20]

3.2 Numerical goniophotometers

LESO-PB / EPFL

The experimental conditions described above were reproduced virtually with the commercial forward ray-tracer TracePro® based on Monte Carlo calculations [21, 22]. The simulation model included a detection screen (made out of 6 panels covering 360°) and a model of each sample as close as possible to the physical elements.

The rays were emitted from an annular grid, composed of 45 rings and sending about 6000 rays at wavelength 555 nm.

FHG-IBP

The FHG-IBP Numerical Goniophotometer represents an automated environment allowing a virtual test set up to be configured, CFS samples to be parameterized and combined, and includes a post-processing of data for further use in daylight simulation [10, 23]. The environment is based on the commercial forward ray-tracing tool OptiCad™ and uses a flux-based method [24]. Generators for different kinds of CFS (like prismatic elements, laser cut panels, venetian blinds, etc.) are provided.

3.3 BTDF datasets and related error sources

The BTDF of both the Serraglaze™ and the Laser Cut Panel were determined experimentally with the bidirectional video-goniophotometer and were calculated with both numerical

goniophotometers. The samples were numerically modeled according to the manufacturer's specifications.

While the BTDF datasets of both the Laser Cut Panel and the Serraglaze™ showed very close qualitative behaviors between measured and simulated values, the hemispherical transmission values deduced from measurements were significantly lower than for both simulated datasets. For the Laser Cut Panel, these differences were attributed to manufacturing irregularities. The Serraglaze™ showed larger differences between measured and simulated data, which most likely were related to incorrect assumptions on geometry and material of the simulated sample, in addition to the inevitable manufacturing inaccuracies [21, 22, 25]

A quantitative analysis of the errors associated with BTDF data measurement or calculation is given in reference [10]. Overall, errors on BTDF varied between 10% and 15%.

4. Applied simulation methods

Two types of simulation approaches at the room level were tested: simulations using BTDF data for the glazing and simulations based on ray-tracing only (Radiance-based simulations). Below, a description of these methods is presented in addition to a discussion about the related error sources.

4.1 Simulation methods using BTDF data

The common procedure for the BTDF-based simulations is to combine the measured or calculated BTDF data with the exterior luminance distribution to calculate a resulting inside flux distribution.

4.1.1 Equivalent luminaire method - ENTPE

The ENTPE method for CFS simulations is based on replacing the sample inner surface by an equivalent luminaire associated to a given intensity distribution, which is obtained from the Photolux sky luminance map and the LESO-PB/EPFL measured BTDF data.

To create the equivalent intensity distribution, the 360,000 luminance values from Photolux were first reduced to 145 values representing the average luminance of the 145 sky sectors (covering the whole hemisphere) corresponding to the incidence directions for which the BTDF data had been measured.

For each of these 145 sectors, the resulting illuminance on the sample surface was calculated and multiplied by the corresponding BTDF value along every transmission direction (every 5 degree in azimuth and zenith) to obtain the transmitted luminance in these directions.

The total transmitted luminance along each transmission direction was obtained by adding the 145 transmitted luminances due to each of the 145 sky sectors. These total luminances were then transformed into intensity values that were saved into an intensity distribution file using the standard IESNA format. This file was then used to conduct a lighting simulation within Autodesk Lightscape 3.2, a commercial program that has a referenced high accuracy for direct artificial lighting simulations (error less than 1%) and for diffuse inter-reflections (error less than 3% for a surface reflectance between 0 and 80%) [16].

For the empty opening case, the simulations were based on the intensity distribution files produced by Photolux from the measured luminance maps (1° resolution).

Up to one hour was needed to prepare the simulations while a few minutes were needed for the execution including the production of the intensity distribution file.

4.1.2 CFS algorithm - FHG-IBP

The algorithm used at FhG-IBP is independent of specific lighting simulation programs and can be incorporated into different standalone tools (e.g. CFS database, lighting simulation engine) [26].

The main difference between this method and the previous one is that it uses special “filters” to pre-process raw BTDF data and avoids artifacts in the obtained candlepower distribution. Such artifacts result from the fact that the data resolution on the incident side (145 points) is usually significantly lower than the resolution on the emerging hemisphere and are illustrated in Figure 10. The filtering procedure is explained in more detail in reference [26].

Figure 10

For this study an implementation of the method into the RADIANCE program system was used. CFSs were computed based on both measured (LESO-PB / EPFL) and simulated (FHG-IBP) BTDF datasets.

Raw BTDF data have to be preprocessed (filtered) only once. They are then stored in a separate format, which makes the CFS systems quickly available for future simulation runs. The filtering process takes a couple of minutes. From the filtered data the intensity distribution for a specific sky distribution is obtained within seconds. As for the ENTPE method, the preparation of the simulation set-up itself took about one hour.

4.1.3 DELight

DELight is a general-purpose, radiosity based, daylighting analysis tool [27, 28]. The procedure followed to obtain the results for this study can be described as following:

The CFS aperture surface was gridded to 20x20, interior wall surfaces were gridded to 60x80, and the floor interior to 80x80.

The LESO-PB/EPFL BTDFs were pre-processed into an internal DELight data representation, preserving the incident (Tregenza) directions and with a transmitted resolution based on 1250 equally distributed angular directions. Those pre-processed BTDFs were then used with the Radiance sky files in a sky-BTDF integration, to produce a directional luminance map of the light transmitted through the CFS in the aperture into the test box. This part of the process is similar to the ENTPE equivalent Luminaire method.

Internal surfaces were not defined for 36 mm high edges of the finite-depth aperture. The actual aperture opening height was assumed to be 636 mm above the floor for the empty opening and 643 mm when the CFS was placed over the aperture. DELight instead uses an approximate “Reveal-depth” algorithm.

Because of the low (4.5%) internal surface reflectance, the inter-reflection calculations were limited to a “one-bounce” approximation, i.e. the reflected luminance from a point on a surface was calculated only from direct aperture illuminance on that point.

Initial attempts to use the full datasets and specifications for comparisons led to the realization that there were ambiguities, minor errors, and gaps which had to be repaired before the final comparisons could be made. This was accomplished through an iterative, interactive process between all participants, both the data providers and the data users. These efforts led to a final consensus dataset that matched the experimental situation as closely as possible.

Preparation time thus exceeded one hour due to the complexity and high level of detail in the specifications necessary to accomplish the comparisons. The execution time for a single DELight analysis for the resolutions used for the sky, the BTDF, the number and location of surface illuminance reference points, and the surface meshes were however less than a minute each.

4.2 Ray-tracing based model (Radiance)

This method is based on a calculation algorithm developed to model and simulate LCP in Radiance. The LCP transmits and reflects incident light rays, generating three possible emergent rays: reflected, deflected and undeflected. For each ray incident upon an LCP, a linked function file calculates the fractions reflected, deflected and un-deflected, and the directions of these emergent beams [29].

The LCP was modeled in Radiance using the prism2 material primitive. This material primitive is used to simulate light redirection from prismatic glazing. Using this algorithm, it is possible to model any LCP geometry, as long as the cuts are normal to the panel surface. The model treats the LCP as a macroscopic entity of homogeneous light redirection properties, rather than a microscopic entity comprising several small air gaps. Multiple internal reflections and internal losses are considered. Two ray redirections are passed to the output, those being the most important of the three possible components.

LCP simulations were performed using Radiance (Desktop Radiance v2.0). The material has a refractive index of 1.49 and D/W ratio 0.66667 (thickness 6mm, cut spacing 4mm). High quality simulation parameters were created, with ambient calculation parameters -ab 6 -aa .125 -ad 512 -as 256 -av 0 0 0. Simulations took little time to complete, requiring calculation times less than 3 minutes for each analysis.

4.3 Error analyses

4.3.1 Errors with BTDF-based indoor illumination assessment methods

Because of the many similarities found in the three methods using BTDF data, common error sources could be identified:

- Data interpolation at different levels: sky luminance map, BTDF output resolution, and calculated intensity or luminance distribution.
- BTDF-sky integration. The related error was mainly due to the difference in resolution between the BTDF input measurements and the sky luminance distribution. This usually led to “spiky” or “bumpy” luminance maps (i.e. abrupt changes in the simulated luminance distribution for the CFS. see Figure 10) introducing errors in the simulation results. The filtering method in FHG-IBP’s approach allowed a solution to be found for smooth (low frequency) sky luminance distributions and this, independently of the type of BTDF (low frequency as for diffuse glazing as well as high frequency (i.e. including peaks) as for LCP and Serraglaze). When both the sky distribution and the BTDFs involved high frequency components, the error in the final intensity distribution can increase at high resolution [26].

Other error sources specific to each method could also be predicted, for example those related to the reveal-depth algorithm applied by DELight, or to the accuracy parameters defined in each of the tested methods.

In addition to these method-related error sources, other errors can be expected in relation to the accuracy of the BTDF (described in 3.3) or to the light propagation inside the buildings (inter-reflections, obstructions, etc.)

4.3.2 Errors with Radiance-based indoor illumination assessment methods (LCP model)

The Radiance lighting simulation tool has been subjected to numerous validation exercises [27, 30, 31, 32, 33]. Radiance simulations compared very well with measurement for both simple and complex geometries, providing errors generally less than 15%.

However, some additional error can be expected for this study, related to the simplified laser cut panel modeling algorithm. The extent of this additional error has been estimated to 5% through comparison of simulated and measured luminous transfer efficiencies [34].

5. Comparison between simulation results and measurements

For both scenarios, simulation results were based on a combination of contributing institutions and methods:

- DELight simulations: simulations performed at LBNL using the DELight simulation tool and based on LESO-PB/EPFL measured BTDF data
- ENTPE simulations: Lightscape simulations performed at ENTPE employing the equivalent luminaire method based on LESO-PB/EPFL measured BTDF data

- FHG-IBP simulations with measured BTDFs: Simulations performed at FHG-IBP using Radiance - integrated CFS algorithm, and using BTDF data measured at LESO-PB / EPFL
- FHG-IBP simulations with calculated BTDFs: Simulations performed at FHG-IBP using Radiance-integrated CFS algorithm, applying BTDF determined by the FHG-IBP numerical goniophotometer
- Radiance simulations: Radiance LCP simulations employing analytical LCP modeling algorithm

5.1 Serraglaze™ scenario

Simulation results for the Serraglaze™ scenario are illustrated in Figure 11. A few general comments can be made:

Bare opening results (see A1 and A2 of Figure 11): A good agreement with reference data was generally observed for the majority of the simulation results, as these were either within the tolerance bounds or very close to the lower boundary (within a margin of 20%). The exceptions were for DELight results at the upper wall point (30% difference with the measurement, see A2 of Figure 11).

Serraglaze results (see B1 and B2 of Figure 11): A good agreement with reference data was generally observed for the DELight and FHG-IBP measured BTDF results, but not for the FHG-IBP calculated BTDF and ENTPE results. Same as for the bare opening, DELight results again showed less agreement at the wall points (within a margin of 25%).

Figure 11

5.2 LCP Scenario

Simulation results for the LCP scenario are illustrated in Figure 12. The reference data of the LCP scenario were particularly interesting as the re-directional effect of the CFS could be highlighted thanks to the strong directionality of the sky luminance map. Figure 13 shows the effect of the LCP where it enhanced the uniformity of the illuminance on the floor (compared to the case of empty opening).

Bare opening results (see Figures 12(A1) and 12(A2)): Except for the prediction provided by the FHG-IBP at the wall upper point (30% difference with measurement), a good agreement with the reference data was observed for almost all simulation results (only 2 values obtained by each of FHG-IBP and Radiance methods at the floor exceeded the error margins, but remained within a 20% range). For the higher illuminance values (floor point 5 to floor point 7) all simulation results are very close and lie rather close at the lower error bound.

LCP results (see Figures 12(B1) and 12(B2)): All methods gave results within or very close to the tolerance bounds except for the ENTPE simulation where illuminance values were under-predicted at floor points 5 to 7 (up to 45% difference with measurement) and the floor illuminance profile was not respected (see Figure 12(B1)). It could also be noted that Delight and Radiance results correlates with the measurement profile better than those of FHG-IBP. IBP (and Delight) results nevertheless reflect the tendency observed for the bare opening, of simulation results being rather close to the lower error bound.

Figure 12, Figure 13

5.3 Results analyses

Based on the results and the observations presented above, the following analyses were made:

- Except for the few exceptions mentioned above, all simulation results fits within a 20% error margin, which can be considered as acceptable accuracy for design work (especially if compared to the high dynamism of daylight).
- The poorer agreement between FHG-IBP measured BTDFs and FHG-IBP calculated BTDFs for the Serraglaze scenarios were attributed to the difference in the original BTDF

data. This difference seems to be mainly due to an inaccurate description of the sample, as this description could not be confirmed by the manufacturer.

- The disagreement between measured and Delight-simulated results for the upper wall point for the Serraglaze scenarios were attributed to the approximations made on the window reveal-depth algorithm.
- The ENTPE method failed to simulate, with an acceptable accuracy, the influence of the LCP on the internal illuminance. This is probably due to a wrong orientation in the calculated intensity distribution file or to its bumpiness, as discussed in sections 4.1.2 and 4.3. The reliability of the method needs to be assessed further.

6. Conclusions

The applied validation approach showed to be useful in assessing the capabilities of the tested simulation methods in predicting the performance of CFS under given sky conditions. The simplicity of the test cases allowed us to more easily identify the error sources of the simulation methods. However, due to this simplicity, the conclusions of this work cannot be generalized to more complex scenarios like for example with direct sun.

The results of this study proved the capability of most of the tested methods to quantitatively simulate CFS light distribution effects in the room: Overall, the comparison of reference data and simulations showed acceptable results: in most cases, predicted data fell within the range of measurement error (10-20%). A few difficulties were observed but could not be explained (e.g. FHG-IBP wall point result (bare opening) and ENTPE floor results (with sample) for the LCP scenario). However, given the complexity of the CFS materials and of the simulation algorithms involved, these results are encouraging and the achieved level of accuracy for most methods was considered to be acceptable for design studies.

It should be noted that the required level of accuracy varies with the type of application. This study could not point out one of the assessment methods as clearly more appropriate or accurate, as the uncertainties in the experimental reference data were significant (physical properties of samples, artificial/real sky luminance distribution, illuminance measurements, BTDF data). However, depending on the user preferences and type of applications, each one shows easily identifiable strengths and weaknesses:

- DELight presents the advantage of having only one tool to use for the complete daylighting simulation procedure.
- Being based on the calculation of intensity distribution files, the FHG-IBP tool has the advantage of flexibility where it can be used as a plug-in with any existing daylighting and artificial simulation tool.
- The ENTPE tool based on the production of equivalent photometric files in IESNA format has also the advantage of compatibility with any type of lighting simulation programs including artificial lighting tools. However, further validation work needs to be done to confirm the reliability of the method.
- The Radiance algorithm has the advantage of avoiding the need for BTDF data, but is limited to a given type of CFS.

This work also showed the importance of an accurate description of the CFS, whether for ray-tracing simulations or for methods using calculated BTDFs. On the other hand, the resolution in incidence and transmission for measured and calculated BTDFs proved to be an important issue in itself.

It was shown that calculated BTDF data could be used to replace experimental BTDF measurements as long as the CFS consist of an assembly of optical materials for which there is a reliable description. For other types of existing CFSs (e.g. those including partially diffusing components such as Venetian blinds), the reliability of the BTDF simulation methods still has to be proven, as measurements will be necessary to describe the materials/coatings anyway.

The overall goal of this study was to determine whether an agreement between algorithmic approach and measurements was good enough to lead to easier and useful real-world design analyses. This paper describes an encouraging outcome of this work, but further validation data would be needed to confirm the reliability of the applied methods and would help understanding some of the observed weaknesses.

Some recommendations can be made for further analyses:

- For future validation data, it would be useful to measure and use internal luminance maps as reference data for comparison with simulation results.
- As only diffuse sky luminance distributions have been studied, further validation for the direct component would be desirable. Indications on the performance of BTDF-data based algorithms under direct illumination can be found in [26].
- The use of higher resolutions in assessing BTDF (on the incident side) should be considered to avoid related error sources, especially as the time and cost associated to determine BTDF data are decreasing thanks to new developments.

The use of BTDF based simulation methods should be optimised through developing a wide BTDF database for existing CFS. Such a database has already been initiated by IBP [10], but it needs to be populated with further data.

7. Acknowledgements

This work was realized within the framework of Task 31 of the International Energy Agency (IEA), Solar Heating and Cooling Programme (SHC).

8. References

- [1] Ballinger, J. and Lyons, P. (1998). Advanced glazing and associated materials for solar and building applications. Report for IEA SHC Task 18, Draft Final Report for Subtask A.
- [2] International Energy Agency (2000). Daylight in Buildings - A source book on daylighting systems and components. IEA SHC Task 21 / ECBCS Annex 29, Berkeley.
- [3] Kischkoweit-Lopin, M. (2002). An overview of daylighting systems. *Solar Energy*, 73(2):7782.
- [4] Scartezzini, J.-L., Compagnon, R., Ward, G., and Paule, B. (1994). Computer daylighting simulation tools. Technical report, University of Geneva / EPFL, Lausanne.
- [5] Reinhart, C. and Herkel, S. (2000). The simulation of annual daylight illuminance distributions a state-of-the-art comparison of six RADIANCE-based methods. *Energy and Buildings*, 32(2):167–187.
- [6] Roy, G. (2000). A comparative study of lighting simulation packages suitable for use in architectural design. Technical report, Murdoch University, Perth, Western Australia.
- [7] Mitchell, R., Kohler, C., Arasteh, D., Carmody, J., Huizenga, C., and Curcija, D. (2003). THERM 5 / WINDOW5 NFRC Simulation Manual. Window & therm documentation, Lawrence Berkeley National Laboratory, Berkeley, CA.
- [8] Commission Internationale de l'Eclairage (1996). The photometry and goniophotometry of luminaires. CIE, 121.
- [9] Commission Internationale de l'Eclairage (1977). Radiometric and photometric characteristics of materials and their measurement. CIE, 38(TC-2.3).
- [10] Andersen, M., de Boer, J. (2006) Goniophotometry and assessment of bidirectional photometric properties of complex fenestration systems. *Energy and Buildings*, In Press.
- [11] Mitanchey, R., Escaffre, L., and Marty, C. (2002). From optical performances characterization of a redirecting daylight material to daylighting simulations. In Proceedings of the 3rd European Conference on Energy Performance & Indoor Climate in Buildings EPIC 2002, pages 721–726, Lyon, France, Oct. 23-26. ENTPE.
- [12] De Boer, J. (2003). Incorporation of numerical goniophotometry into daylighting design. In Proceedings CISBAT 2003, pages 229–234, Lausanne, Oct. 8-9. EPFL.

- [13] Maamari, F., Fontoynt, M. (2002). Use of IEA-SHC Task 21 C benchmarks to assess performance of Lightscape 3.2 in daylighting calculations. In: Lyon, France, Proceedings of EPIC conference, pp. 709-714.
- [14] Commission Internationale de l'Éclairage (2004). Test cases to assess the accuracy of Lighting computer programs, Under review.
- [15] Slater, A., Graves, H. (2002). Benchmarking Lighting Design Software. TM 28/00. London: CIBSE, 2002, 33 p.
- [16] Maamari, F. (2004). Simulation numérique de l'éclairage, limites et potentialités. PhD in Civil Engineering. INSA de Lyon, Lyon, 280 p.
- [17] Coutelier B., Dumortier D. (2003). Luminance calibration of the Nikon Coolpix 990 digital camera. In Proceedings of the 25th Session of the CIE, San Diego, 2003, Vol. 1, D3-56.
- [18] Mardaljevic, J. Quantification of Parallax Errors in Sky Simulator Domes for Clear Sky Conditions Lighting Res. Technol. 34(4) 2002, pp 313-332
- [19] Andersen, M., Michel, L., Roecker, C., Scartezzini, J.-L. (2001) Experimental assessment of bi-directional transmission distribution functions using digital imaging techniques. Energy and Buildings 33 (5): 417-431.
- [20]. Andersen, M., Roecker, C., Scartezzini, J.-L. (2005) Design of a time-efficient video-goniophotometer combining bidirectional functions assessment in transmission and reflection. Solar Energy Materials and Solar Cells 88 (1): 97-118.
- [21] Andersen, M., Rubin, M., and Scartezzini, J.-L. (2003). Comparison between ray-tracing simulations and bi-directional transmission measurements on prismatic glazing. Solar Energy 74(2):157–173
- [22] Andersen, M., Rubin, M., Powles, R., Scartezzini, J.-L. (2005). Bi-directional transmission properties of venetian blinds: experimental assessment compared to ray-tracing calculations, Solar Energy 78(2):187-198.
- [23] de Boer, J. : Numerical Goniophotometer. User Manual, Fraunhofer Institute for Building Physics, Stuttgart (2004).
- [24] OptiCad: Opticad, Optical Analysis Program User's Guide Version 7.0. Opticad Corporation, Santa Fe (2001).
- [25] de Boer, J. : Tageslichtbeleuchtung und Kunstlichteinsatz in Verwaltungsgebäuden mit unterschiedlichen Fassaden. PhD thesis, Universität Stuttgart, Stuttgart (2004).
- [26] de Boer, J. (2006) Modelling indoor illumination by complex fenestration systems using bidirectional photometric data. Energy and Buildings, In Press.
- [27] Hitchcock, R.J., Carroll, W. L. (2003). DELight: A Daylighting and Electric Lighting Simulation engine, International Building Performance Simulation Association, IBPSA BS 2003, Eindhoven, Netherlands.
- [28] U. S. Department of Energy, (September 2004), EnergyPlus Engineering Document. <http://www.eere.energy.gov/buildings/energyplus/pdfs/engineeringdoc.pdf>
- [29] Greenup, P., Edmonds, I.R. and Compagnon, R. (2000), RADIANCE algorithm to simulate laser-cut panel light-redirecting elements, Lighting Res. Technol., 32(2), 49-54.
- [30] Mardaljevic, J., 1995. Validation of a Lighting Simulation Program under Real Sky Conditions. Lighting Res. Technol., 27 (4), 181-188.
- [31] Mardaljevic, J., 2000. Daylight Simulation: Validation, Sky Models and Daylight Coefficients. Leicester, UK: De Montfort University.
- [32] Mardaljevic, J., 2001. The BRE-IDMP Dataset: A New Benchmark for the Validation of Illuminance Prediction Techniques. Lighting Res. Technol., 33 (2), 117-136.
- [33] Khodulev, A.B. and E.A. Kopylov, 1996. Physically Accurate Lighting Simulation in Computer Graphics Software (World Wide Web site). url: rmp.kiam.ru/articles/pals, accessed: 22 Jan.

[34] Greenup, P.J. (2004), Development of Novel Technologies for Improved Natural Illumination of High Rise Office Buildings, PhD Thesis, Queensland University of Technology, Brisbane.

List of figures

Figure 1. (a) Scale model with the Serraglaze™ sample over the opening surface. (b) Camera positioning system for real sky scenario

Figure 2. Using calibrated photos to produce a luminance map in Photolux

Figure 3. Illustration of the considered complex glazing materials. (a) Laser Cut Panel. (b) Serraglaze™.

Figure 4. Measurement points positions for the Serraglaze™ scenarios

Figure 5. Luminance map for Serraglaze scenario

Figure 6. Sky condition during the LCP scenario

Figure 7. Measurement points positions for the LCP scenario

Figure 8. Illustration of the near field error source

Figure 9. Influence of the near field corrections on the correlation between measurements and simulation results

Figure 10. Influence of filter corrections. Upper figure: Superposition of the *unfiltered* candle power distributions. Lower figure: Superimposed *filtered* candle power distributions.

Figure 11. Serraglaze scenario results

Figure 12. LCP scenario results

Figure 13. Influence of LCP on the illuminance distribution inside the scale model



(a)



(b)

Figure 1. (a) Scale model with the Serraglaze™ sample over the opening surface. (b) Camera positioning system for real sky scenario

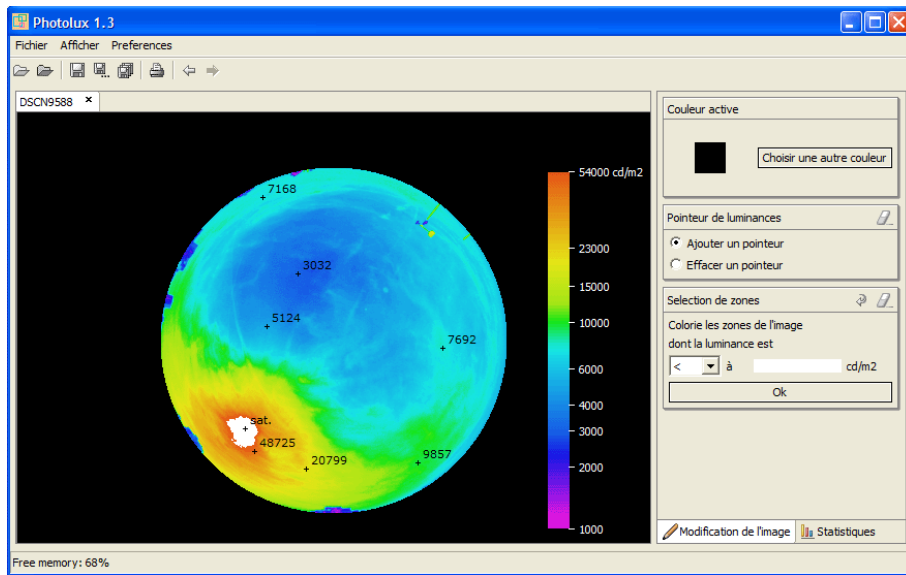


Figure 2. Using calibrated photos to produce a luminance map in Photolux

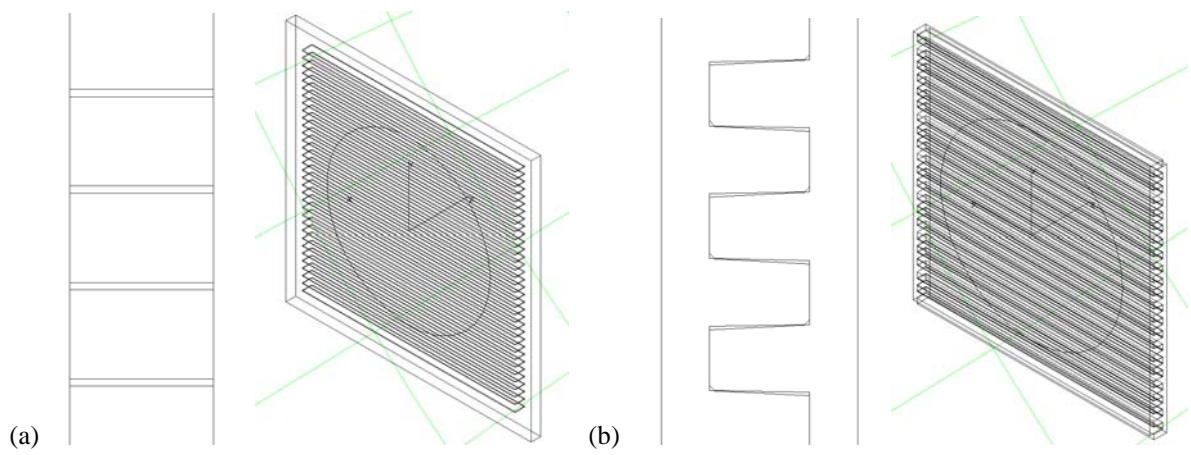


Figure 3. Illustration of the considered complex glazing materials. (a) Laser Cut Panel. (b) SerraglazeTM.

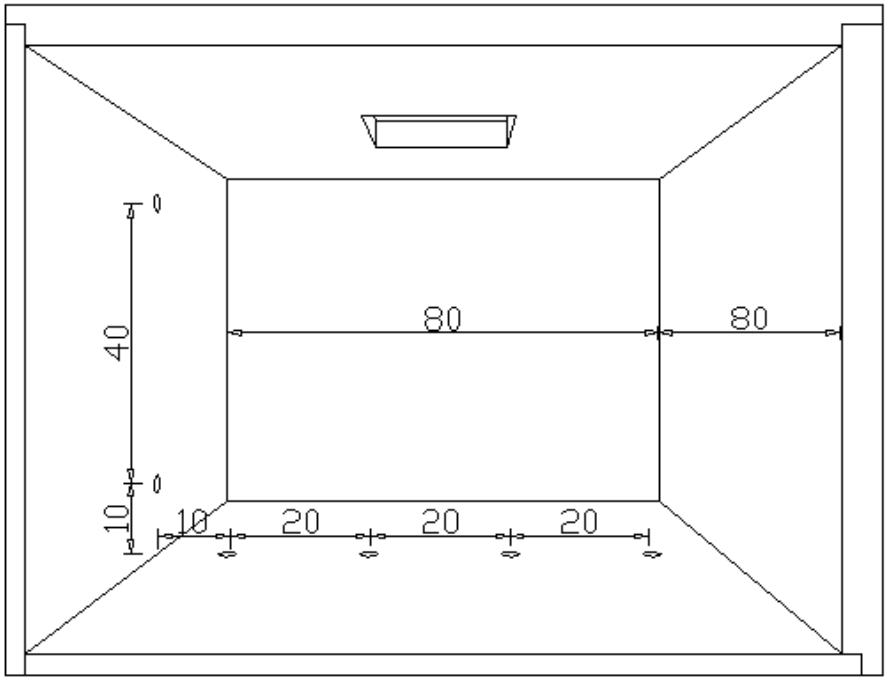


Figure 4. Measurement points positions for the SerraglazeTM scenario (Dimensions are given in cm)

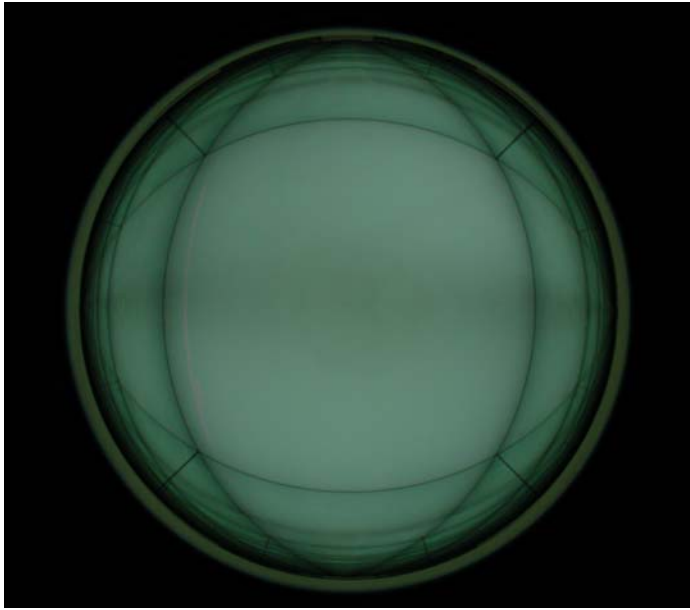


Figure 5. Luminance map for Serraglaze scenario (the lines on the fish-eye view are caused by the mirror box's edges)



Figure 6. Sky condition during the LCP scenario

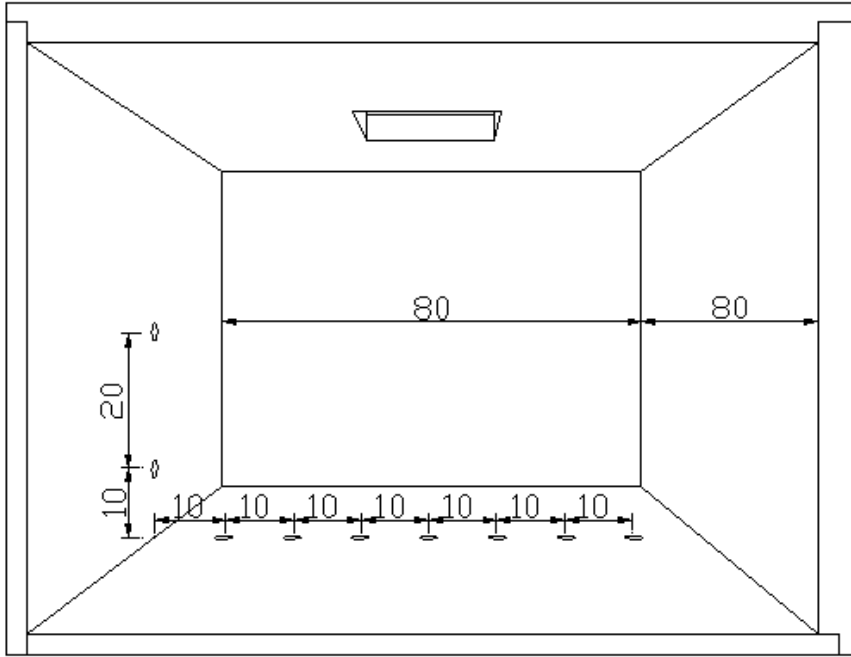


Figure 7. Measurement points positions for the LCP scenario (Dimensions are given in cm)

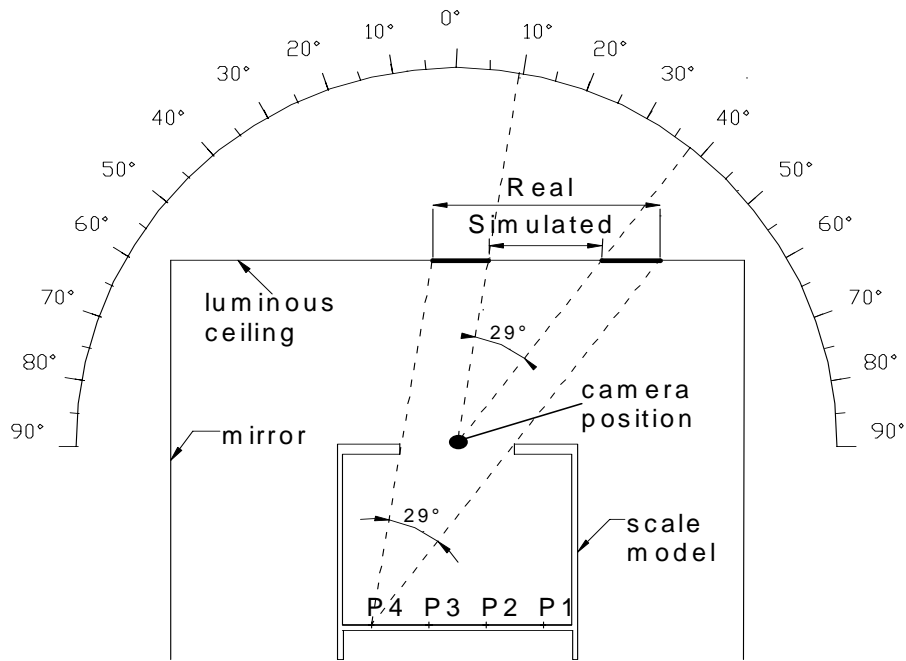


Figure 8. Illustration of the near field error source

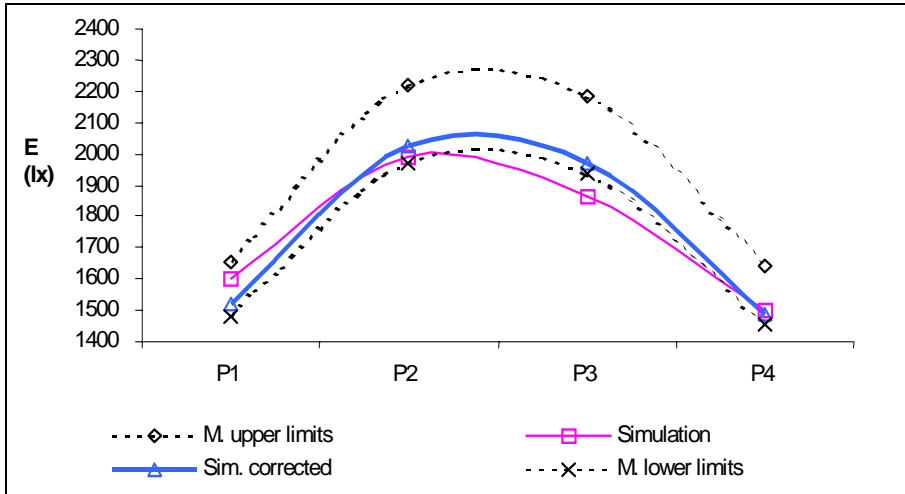


Figure 9. Influence of the near field corrections on the correlation between measurements and simulation results

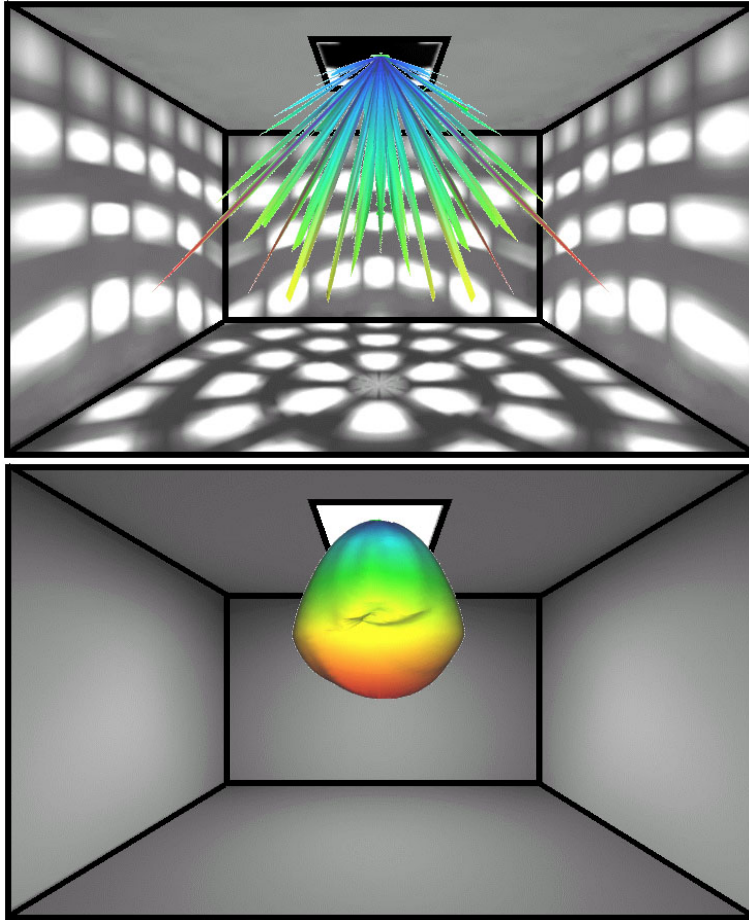


Figure 10. Influence of filter corrections. Upper figure: Superposition of the *unfiltered* candle power distributions. Lower figure: Superimposed *filtered* candle power distributions.

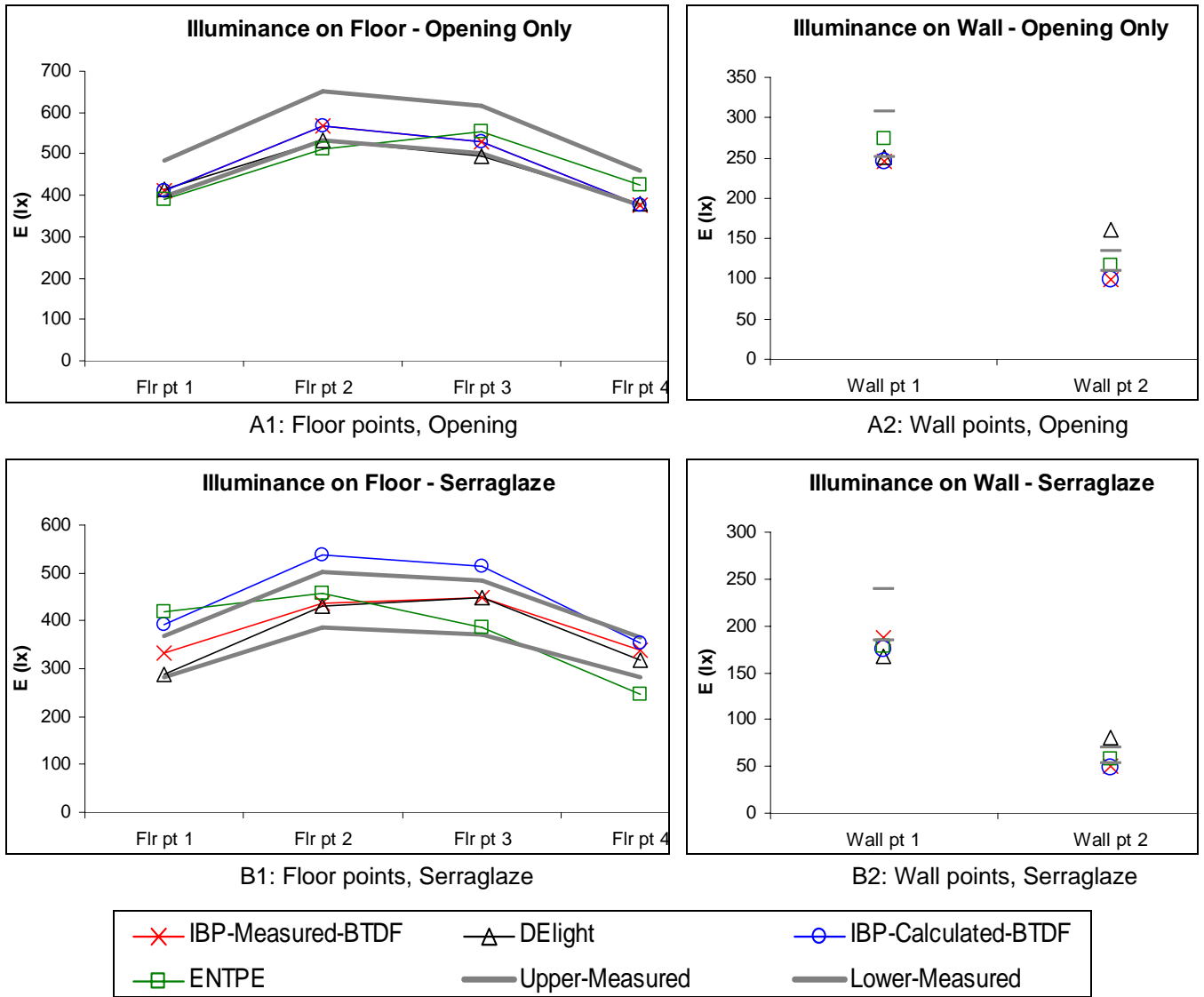


Figure 11. Serraglaze scenario results

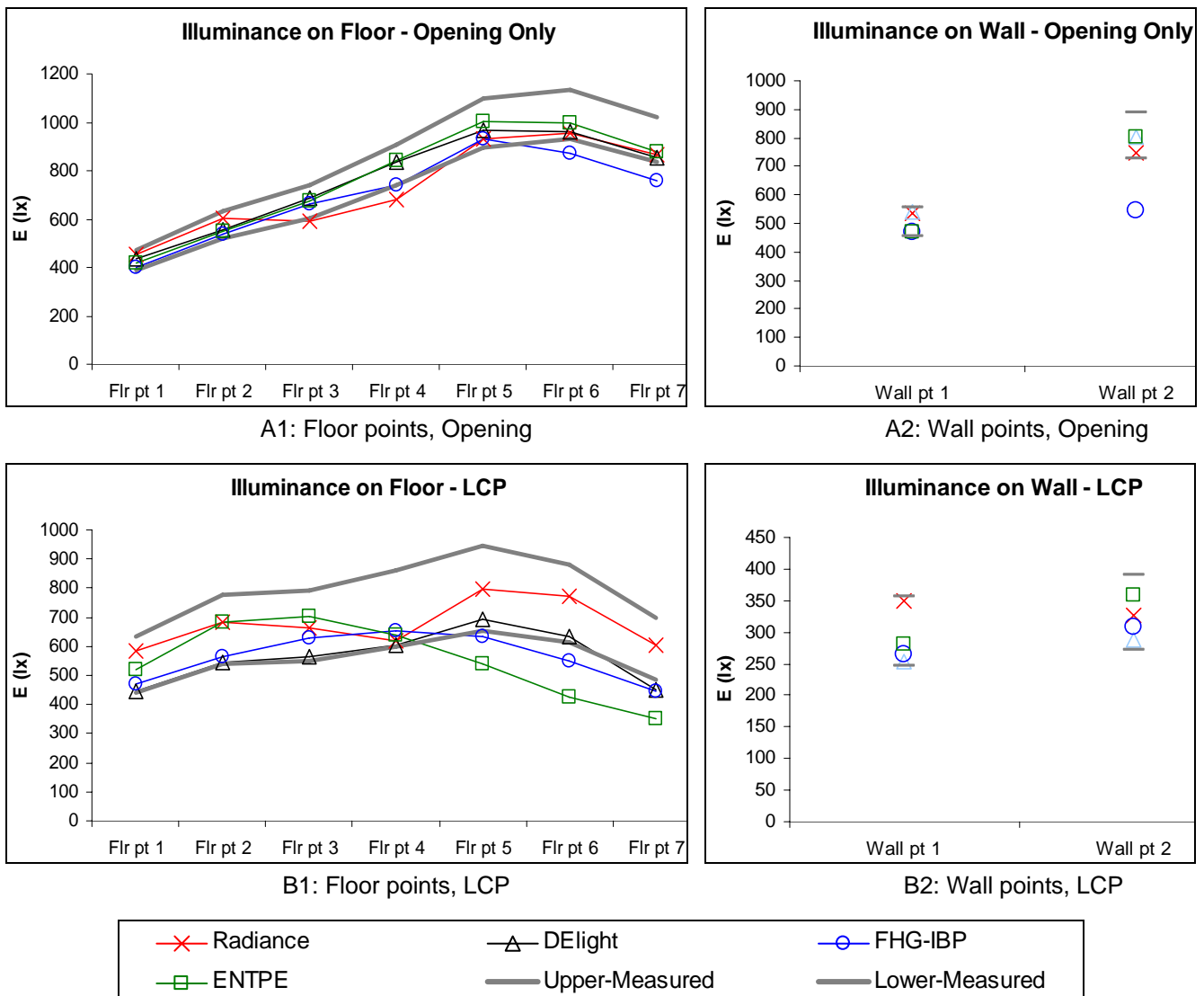


Figure 12. LCP scenario results

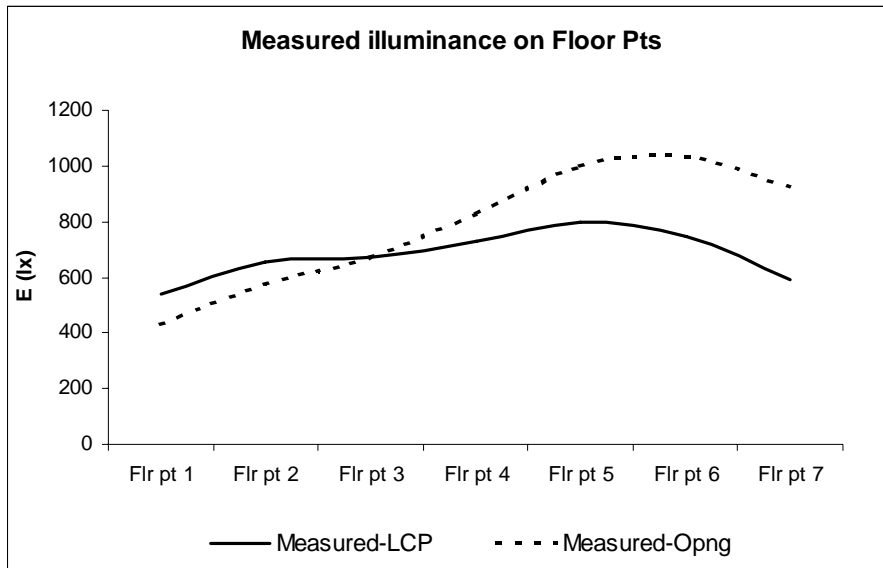


Figure13. Influence of LCP on the illuminance distribution inside the scale model